Figure S1

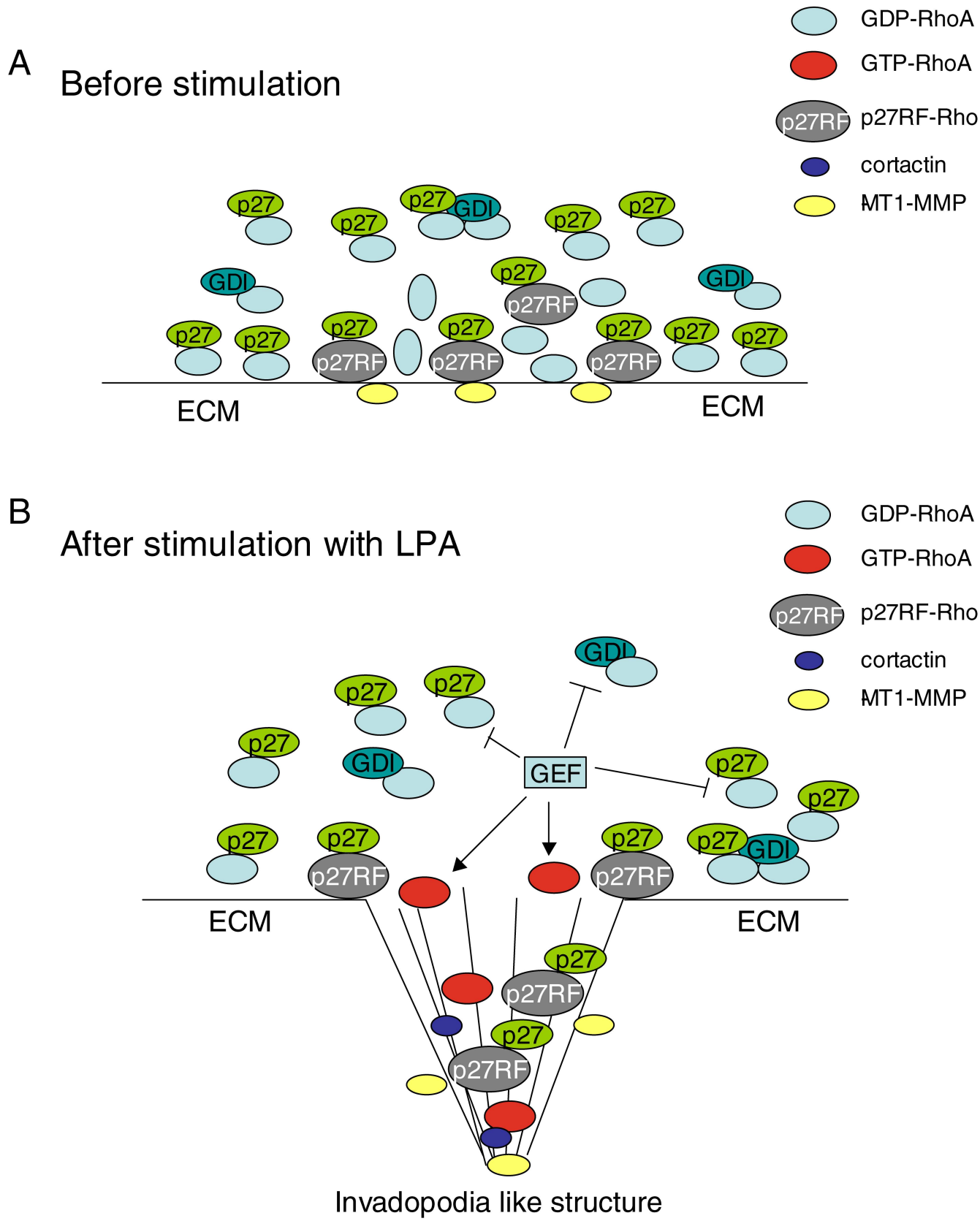

Figure S1. (A), (B) Summary of the p27RF-Rho function and its possible role in invadopodia formation. p27RF-Rho may prepare subcellular area where RhoA can be activated upon stimulation. Interestingly, the distribution pattern of p27RF-Rho resembles that of invadopodia like structure induced by LPA stimulation. Thus, localization of p27RF-Rho may determine the sites of RhoA activation and invadopodia like structure formation. Although cortactin and MT1-MMP are also recruited to invadopodia like structure, the mechanism of recruitment and their order in relation of p27RF-Rho are not known yet.

Figure S2

A

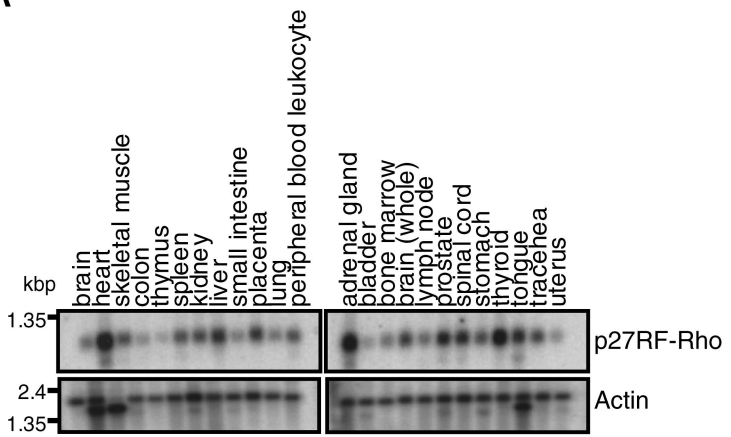

B

Homo sapiens	-
Pongo pygmaeus	98.8 %
Bos taurus	98.1 %
Mus musculus	97.5 %
Rattus norvegicus	96.3 %
Xenopus laevis	70.2 %

Figure S2. Tissue distribution analysis of p27RF-Rho.
(A) Human tissue-derived mRNA samples (clontech) were analyzed by northern blot analysis using a full-length p27RF-Rho cDNA as a probe. (B) Amino acid identity of other vertebrate p27RF-Rho homologues with the human sequence. Accession numbers of the protein sequences in GenBank are as follows : Human (NP_060377), Pongo pygmaeus (CAH92394), Bos taurus (NP_001029941), Mus musculus (NP_079881), Rattus norvegicus (NP_954533), and xenopus laevis (NP_001080198).

Figure S3

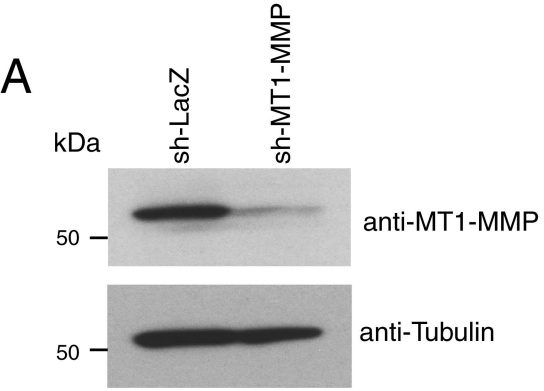

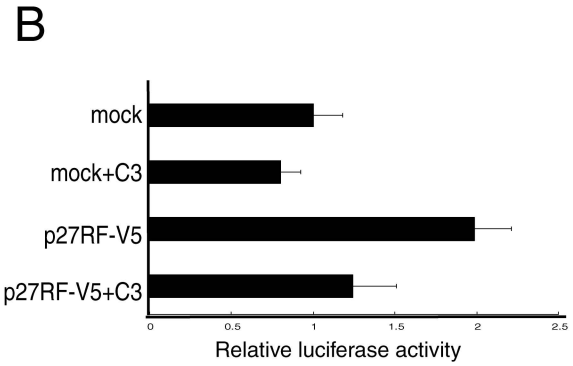

Figure S3. p27RF-Rho enhances expression of MMP9.
(A) MT1-MMP knockdown efficiency was confirmed by western blot analysis.
(B) The effects of the Rho inhibitor C3 on MMP9 luciferase activity.

Figure S4

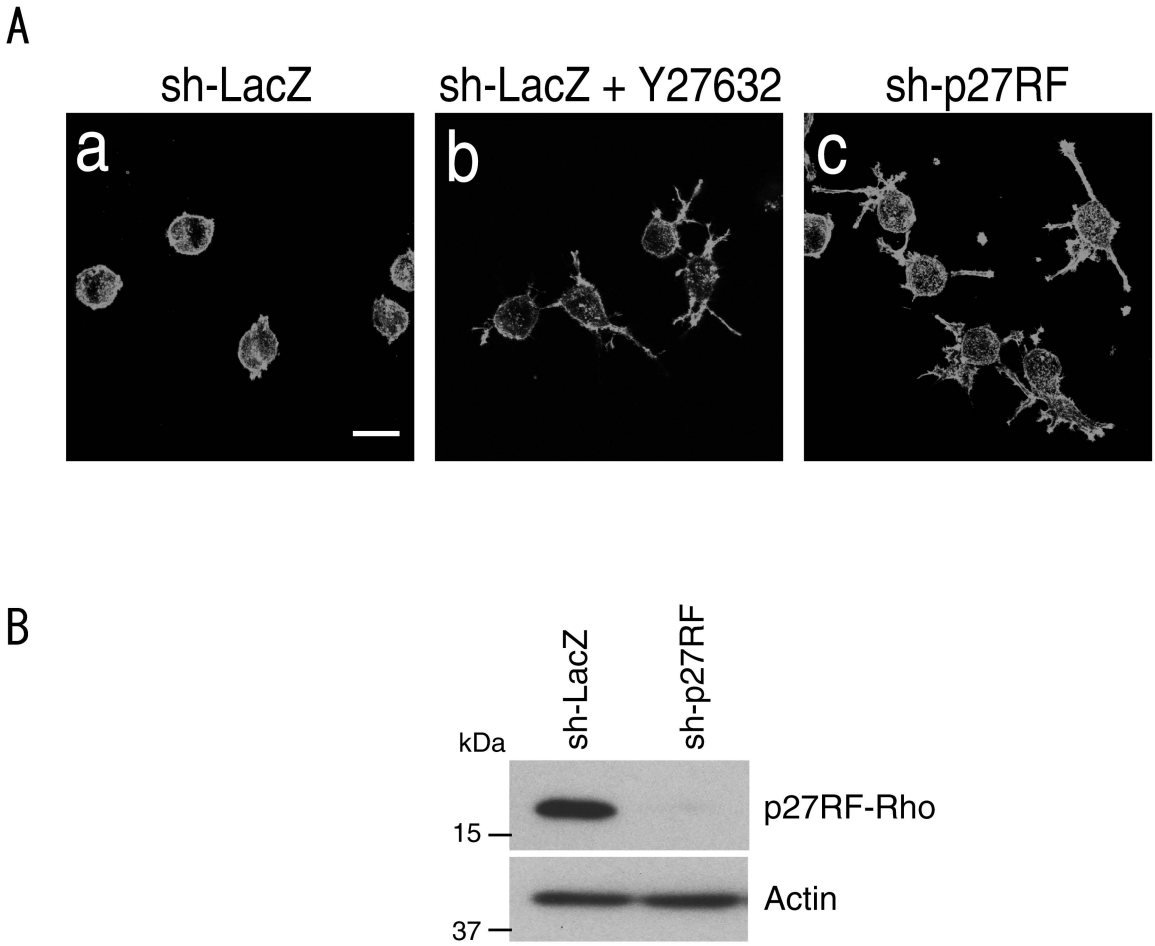

Figure S4. p27RF-Rho modulates cell morphology.
(A) A375 cells stably expressing an shRNA targeting either p27RF-Rho mRNA (sh-p27RF) or LacZ (sh-LacZ) as a negative control were seeded onto collagen/matrigel coated glass coverslips. Actin was visualized with Alexa488-phalloidin. Confocal images using 63 x objective lens (scale bar, 20 μm). (B) Knockdown efficiency was determined by western blot analysis of p27RF-Rho expression compared to that observed in cells transfected with control sh-LacZ targeted lentivector.

Figure S5

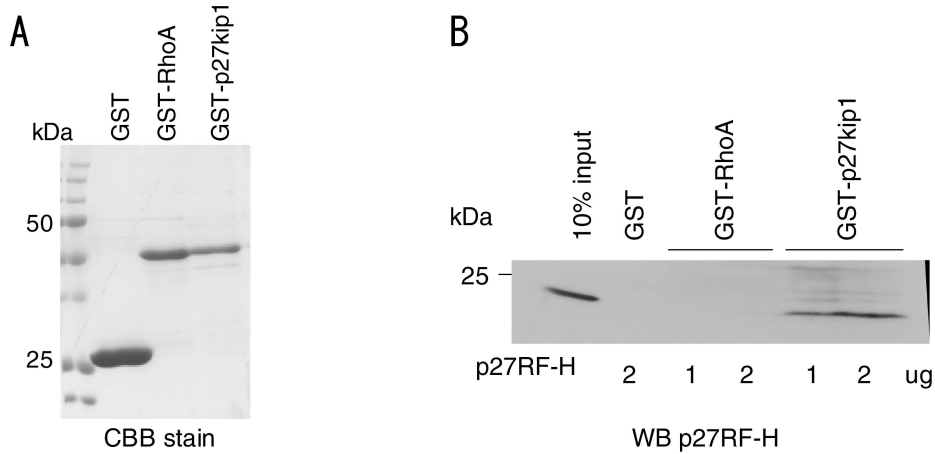

Figure S5. p27RF-Rho directly binds p27kip1.
(A) Recombinant GST, GST-fused RhoA and p27kip1 proteins were analyzed by gel electrophoresis and stained with CBB-R250. (B) Recombinant His-fused p27RF-Rho (p27RF-H) was incubated with either glutathione sepharose conjugated GST, GST-RhoA, or GST-p27kip1, and proteins were pulled down. p27RF-H bound to the GST proteins was detected by western blot analysis.

Figure S6

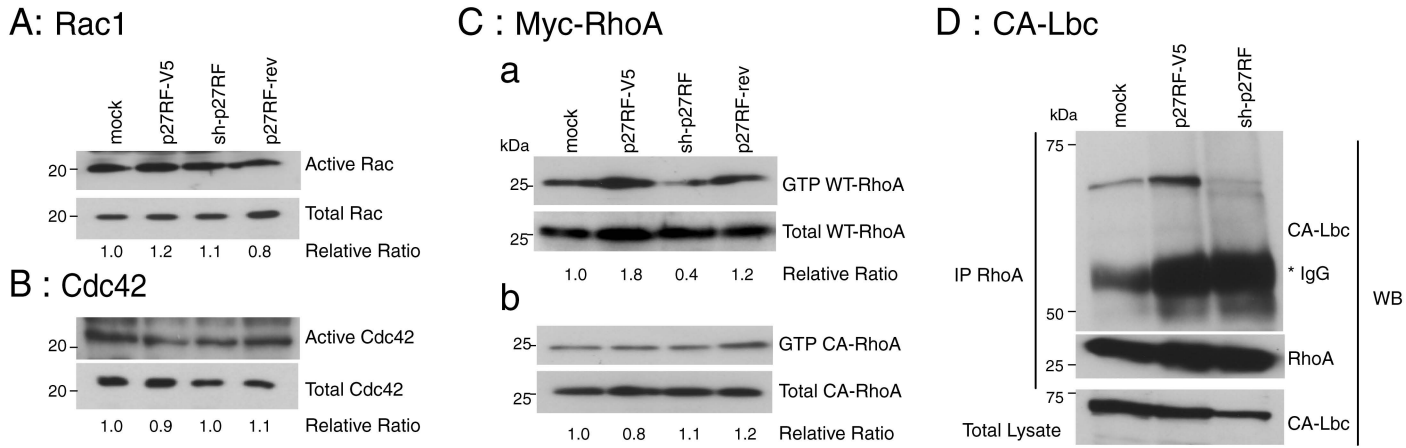

Figure S6. p27RF-Rho promotes the association of GEFs with RhoA

(A,B) GTP-loaded Rho proteins in HT1080 cell lysate were pulled down using GST-Pak for Rac1 (A) and Cdc42 (B). These proteins were detected by western blotting using specific antibodies. (C) HT1080 cells were transfected with an expression plasmid either for wild-type RhoA (a, WT-RhoA) or constitutively active RhoA (b, CA-RhoA) as Myc-tagged forms. The cells were used to analyze the effect of p27RF-Rho on the interaction between Myc-RhoA proteins with GST-Rhotekin. (D) The effect of p27RF-Rho on the association of Myc-RhoA with GFP-CA-Lbc was tested. Myc-RhoA was immunoprecipitated (IP) and associated CA-Lbc was detected by western blot analysis (WB).